SACLANTCEN REPORT
serial no: SR- 325

SACLANT UNDERSEA RESEARCH CENTRE REPORT

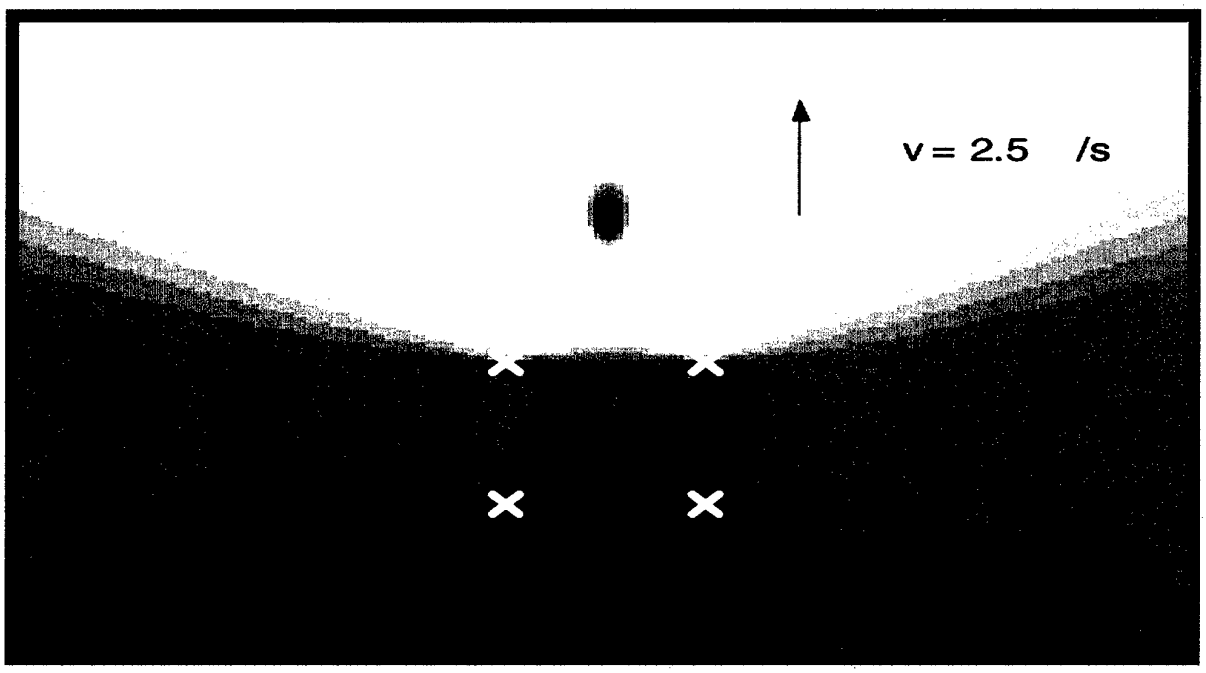

NORTH ATLANTIC TREATY ORGANIZATION ORGANISATION DU TRAITE DE L'ATLANTIQUE NORD

Performance issues concerning Doppler-only localization of submarine targets

I. Levesque, J. Bondaryk

The content of this document pertains to work performed under Project 04-B of the SACLANTCEN Programme of Work. The document has been approved for release by The Director, SACLANTCEN.

Jan L. Spoelstra
Director

intentionally blank page

Performance issues concerning Doppler-only localization of submarine targets

I. Levesque, J. Bondaryk

Executive Summary: Localization and tracking of a target is relevant to research, development and operation of radar and sonar. In sonar technology, bearings-only tracking (BOT) is the traditional method of tracking. In this case, the track of a target with uniform movement is reconstructed from a series of directional and time-of-arrival measurements, requiring an own-ship manoeuvre.

Target localization can be performed using only frequency information. The numerical method proposed is highly accurate when applied to computing target position and velocity from multiple simultaneous Doppler-shift measurements.

The area over which localization can be performed depends on the configuration in which the sensors are placed. The drop-off in performance is step-like. A negligible decrease in performance is encountered when switching from a configuration with *N-source, N-sensors* to a *single-source, N*-sensor configuration.

The number of sensors to be used and the layout configuration are important points to consider in system design.

- Increasing this number beyond 4 is only useful for certain configurations.
- Switching from 4 to 6 sensors decreases the mean localization error by 50%.
- The area over which accuracy is acceptable improves greatly with certain platform layouts.
- Increasing the number of sensors improves results only in certain specific geometrical cases, such as an L-shaped geometry.
- A carefully selected configuration makes the *blind area* predictable.

Uncertainties in the sensor locations decrease the area over which accuracy is acceptable.

- A configuration of six sensors is more robust than a 4-point system when faced with uncertainties.
- Uncertainty of 1 m decreases the coverage area by a few percentage points only.
- Uncertainty of 10 m translates into a 5% loss in coverage.
- Inaccuracy of 100 m reduces the area by 25 to 50% depending on the target variable considered.

The addition of noise to the Doppler information decreases accuracy gradually, as opposed to decreasing the area of accuracy.

- The error on target speed is influenced primarily by noise.
- One can expect a mean error 3 times greater on target speed with the addition of 10% noise.
- Errors in target position and velocity direction are reduced by half with 5% noise, but remain constant with additional noise.

intentionally blank page

Performance issues concerning Doppler-only localization of submarine targets

I. Levesque*, J.Bondaryk

Abstract: Target localization can be achieved using only frequency information obtained from source-receiver platforms. The numerical method proposed is highly accurate in computing target position and velocity from multiple simultaneous Doppler-shift measurements. The area over which localization can be performed depends on the configuration in which the sensors are placed. The drop-off in performance is step-like. A negligible decrease in performance is encountered when switching from *N-source, N-sensors* to a *single-source, N-sensor* configuration. The number of sensors to be used is an important criterion, but more than 4 sensors are only worthwhile with certain configurations. Uncertainties in the sensor locations decrease the area over which accuracy is acceptable; uncertainty of 10 m translates into a 5% loss in coverage. Noise in the Doppler information decreases accuracy gradually; one should expect an error 3 times greater with the addition of 10% noise.

Keywords: Localization, Doppler effect, CW systems, narrow-band systems, Doppler-only localization (DOL)

* Bedford Institute of Oceanography, Halifax, NS, Canada

Contents

1

1. Introduction 1
1.1 *Motivation* 1
1.2 *Previous work* 1
1.3 *Content of Report* 2
2. Problem formulation 4
3. Number of sensors 10
3.1 *Description of the numerical experiment* 10
3.2 *Results* 10
4. Geometry 14
4.1 *Description of the numerical experiment* 14
4.2 *Results* 14
5. Positioning accuracy 21
5.1 *Description of the numerical experiments* 21
5.2 *Random perturbation – all sensors equal* 21
5.3 *Random perturbation – one sensor different* 24
6. Doppler information accuracy 26
6.1 *Description of the numerical experiment* 26
6.2 *Results* 26
7. Single-source configuration 29
7.1 *Description of the numerical experiment* 31
7.2 *Results* 31
8. Conclusions 33
8.1 *Discussion and summary* 33
8.2 *Suggestions for future work* 34
9. Acknowledgements 35
References 36
Annex 37

1
Introduction

1.1 Motivation

The problem of localizing and tracking an underwater target using acoustical information has been addressed in various ways. Data is collected using towed arrays and, drifting or moored sonobuoys.

Passive arrays provide bearing information. Active arrays provide bearing and range information. From bearing and range information and multiple measurements, target tracks can be directly reconstructed. From bearing information alone, target tracks can be reconstructed through bearings-only tracking (BOT).

As buoys, which usually contain a single hydrophone, cannot acquire bearing information, there exists a compromise between range and Doppler shift information. If a pulsed waveform is used, range can be computed, but the broadband signal does not permit Doppler shift evaluation. In the case of a continuous tone waveform (CW) or of a narrow-band signal, the shift in frequency is more easily extracted. Range information cannot be obtained.

The performance of Doppler-only localization (DOL) is investigated in this time-limited feasibility study intended to answer preliminary questions and to shed light on the issues that will have to be resolved.

1.2 Previous work

Localization and tracking of a target is relevant to research, development and operation of radar and sonar. In sonar technology, bearings-only tracking (BOT) is the traditional method of tracking. In this case, the track of a target with uniform movement is reconstructed from a series of directional and time-of-arrival measurements, requiring an own-ship manoeuvre. The problem is well documented, for example by Johnson [1].

The addition of frequency information to BOT modifies the problem to bearings-Doppler tracking (BDT) and has been demonstrated. Passerieux *et al* [2], Jauffret and Bar-Shalom [3], Chan and Rudnicki [4] have studied the problem of BDT, which includes frequency information as a variable.

Using only Doppler information in target localization and tracking is encountered in radar, but much less in sonar. Levanon [5] has worked on active tracking using a source-receiver pair. The method utilizes Doppler shift and its first two derivatives, thus involving multiple temporal measurements. An exact solution to the same problem was subsequently published by Webster [6]. Their work focuses on determining target range, velocity and the angle between the two.

In parallel, the passive problem of tracking a moving radiating target has also been considered. Shensa [7] shows that tracking of a radiating source with constant velocity can be performed using multiple temporal measurements from a single, manoeuvering receiver. Weinstein [8] presents a method for utilizing passive array measurements in localization and tracking. Statman and Rodemich [9], with a single, manoeuvering receiver, compute the rest frequency and minimal distance of approach of the source. Work by Chan and Jardine [10] uses a set of sensors with multiple temporal Doppler measurements to localize and track a non-manoeuvering, radiating target.

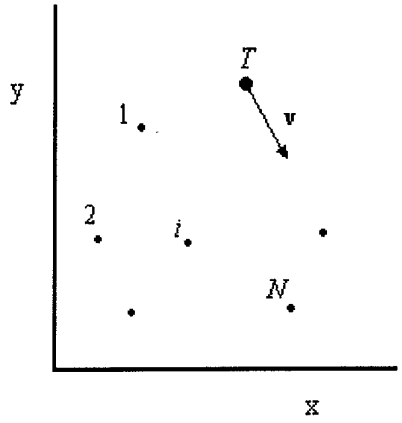

Using Doppler-shift information only, the computation algorithms would apply to the CW or narrow-band active systems previously described. Using an active multiple-sensor layout, it is assumed that simultaneous frequency measurements are obtainable. The objective is to determine target position and velocity from this information and to evaluate the accuracy that is attainable.

Figure 1 shows a typical localization situation, where the smaller points (1–*N*) represent active platforms, *T* the target.

Figure 1 *Problem illustration.*

1.3 Content of Report

Section 2 presents the analytic formulation of the problem. The Doppler effect is presented and the proposed problem is elaborated. The numerical method is explained.

The number of sensors needed to perform localization is considered. Improvements deriving from additional sensors will be extracted, which mathematically corresponds to over-determining the problem (Section 3).

The configuration geometry, i.e. the manner in which the platforms are to be laid out, is examined in Section 4. This is performed for two different numbers of sensors, as determined in the previous section. For these values of N, different configurations are tested to evaluate their performance.

Section 5 examines the problem of platform position uncertainty using a specific geometry and number of sensors. The influence of inaccuracies in platform positioning on the localization results is evaluated. Normally distributed, random perturbations are introduced and localization is performed. The sensors are perturbed equally and unequally to explore the effects of skewing.

Noise is introduced in the Doppler information supplied by the sensors, in Section 6 in order to determine the influence of accuracy of frequency measurements on localization results.

Section 7 describes a system consisting of one source and multiple receivers, to identify potential improvement.

Annex A presents an alternate semi-analytical solution to the particular problem of a target confined to a circle about which N sensors are laid out. It is semi-analytical because it transforms the 4-dimensional numerical minimization problem encountered throughout this work to a 1-dimensional interpolation. This is a proposed solution and tests should be performed using this routine.

2 Problem formulation

The Doppler effect describes the shift observed in frequency due to source and observer movement. A simple one-dimensional derivation is generalized to the full three-dimensional case.

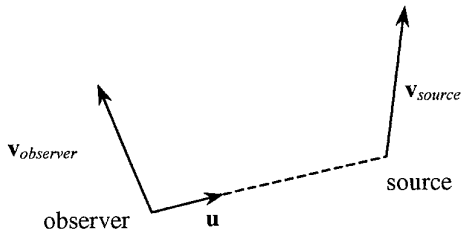

Figure 2 *Source-observer pair.*

Consider the situation illustrated in Fig. 2, where an observer and a source each move with their own velocities. The observed frequency is related to the source's output frequency by:

$$f_{obs} = \left(\frac{c + \vec{v}_{obs} \cdot \hat{u}}{c + \vec{v}_{source} \cdot \hat{u}} \right) f_{source}, \tag{1}$$

where f_{source} is the initial frequency, c is the speed of sound (constant) and $\hat{u}$ is the unit vector point from the observer to the source. From this result, the shift is computed:

$$\Delta f_{Doppler} = f_{obs} - f_{source} = \left(\frac{(\vec{v}_{obs} - \vec{v}_{source}) \cdot \hat{u}}{c + \vec{v}_{source} \cdot \hat{u}} \right) f_{source}. \tag{2}$$

Defining the relative velocity and assuming that speeds are negligible *versus* the speed of sound, the shift becomes:

$$\Delta f_{Doppler} = -\frac{f_{source}}{c} (\vec{v}_{source} - \vec{v}_{obs}) \cdot \hat{u} = -\frac{f_{source}}{c} \vec{v}_{rel} \cdot \hat{u}. \tag{3}$$

The rate of variation of the range from source to observer is equal to the projection of the relative velocity on the unit vector $\hat{u}$. Thus, the shift depends on the rate of variation of the range between source and observer, the initial frequency and the speed of sound:

$$\vec{v}_{rel} \cdot \hat{u} = \frac{dr}{dt} \tag{4}$$

Thus,

$$\Delta f = -\frac{f_{source}}{c}\frac{dr}{dt}, \tag{5}$$

where f_{source} is the initial frequency, c is the speed of sound (constant) and r is the range separating source and observer:

$$r = \left|\vec{r}_{source} - \vec{r}_{obs}\right|. \tag{6}$$

The objective is to localize an underwater target using only the Doppler information in the signal received. It is assumed that sensors can measure frequency shifts to a given accuracy and that reflection off a given target is sufficient to permit data extraction. It will be determined if it is possible to compute the position and velocity of a target from simultaneous measurements and how well this can be achieved. By using Eq. (5), it is hoped that localization of the target can be achieved.

The area to be surveyed is described by a two-dimensional plane. N sensors that perceive only frequency information are laid out on this plane. The problem may be passive, in which case, the initial frequency needs to be determined, or active, in which case the output frequency is known and the shift is measured on the echo.

In the active case, two configurations are considered: multiple sensor-receiver platforms and a single-source, multi-receiver layout. In the first active case, the echo is affected by double the Doppler shift. In the second case, a slightly more general derivation is necessary, to account for source-to-target and target-to-sensor shifts. The former is treated in Sections 3 through 6, the latter in Section 7.

The Doppler shift perceived on echo by a single sensor located at the origin is illustrated as a function of target position in Fig. 3. The shift is plotted as a percentage of output frequency. Target speed is 2.5 m/s heading north, i.e. in the y-axis direction. Frequency shift is plotted for a different target velocity direction at 69° from north in Fig. 4. Sound speed is 1490 m/s. The white cross indicates the sensor.

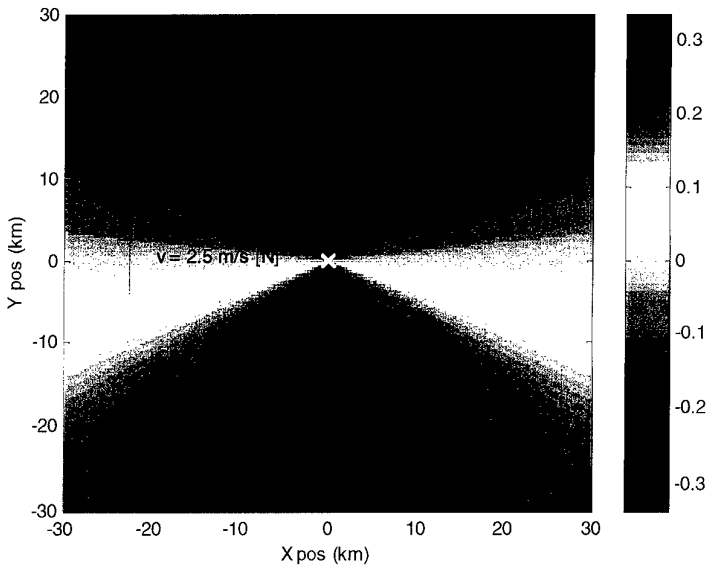

Figure 3. *Doppler shift on echo (% of output frequency).*

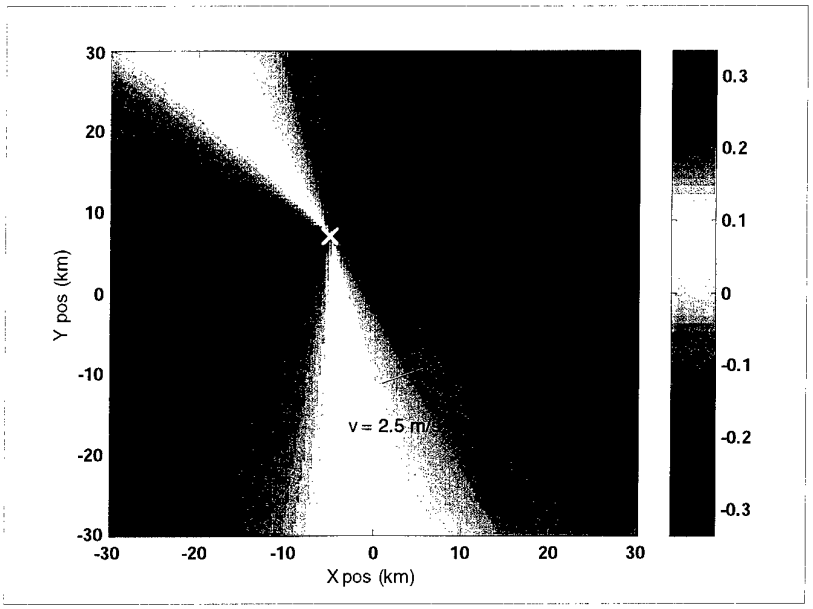

Figure 4 *Doppler shift on echo (% of output frequency).*

These figures illustrate that the frequency of the echo received by the observer will be shifted depending on the movement of the target. The shift can be positive, Up-Doppler, for a target approaching the sensor, or negative, Down-Doppler, for a target moving away from the sensor.

Analytical approach and minimum number of sensors

To solve this problem analytically, one needs to consider that four variables are to be determined. Four equations are theoretically necessary to completely determine the problem. Hence, to supply four independent equations, four points of Doppler information are needed from four platforms.

The equations are non-linear and have the following form:

$$\Delta f_i = -\frac{f_{source}}{c}\frac{(\dot{x}_T - \dot{x}_i)(x_T - x_i) + (\dot{y}_T - \dot{y}_i)(y_T - y_i)}{\sqrt{(x_T - x_i)^2 + (y_T - y_i)^2}} \quad , \tag{7}$$

in Cartesian coordinates, where the i subscript indicates the sensor, $i = 1..N$. In certain cases, such as for static sensors, the equations simplify. This mathematical problem is complicated and no simple solution was found. Specific cases could be considered as in Annex A.

Numerical approach

A simple, closed form solution being difficult to find, one turns to numerical methods in order to perform the localization. An error function in the four-dimensional (x, y, v_x, v_y) space is minimized to obtain the true target state vector. The error function is a sum of squares (SSE) of the difference between Doppler information for a position estimate and true Doppler information:

$$SSE = \sum_{i=1}^{N} \left(f_i^{(true)} - f_i^{(est)} \right)^2 , \tag{8}$$

Here, f_i is the Doppler information vector for the i-th sensor.

The error function is illustrated on the following page. The true target is located 15 km north of the origin, at [0, 15] velocity 2.5 m/s [north], [0, 2.5]. The white crosses indicate sensor locations. Figure 5 shows error in dB against position, for constant velocity. Figure 6 plots error against x-y velocity, in dB. Colour scale is in dB re 1Hz. The minimum is located at the true target position and velocity.

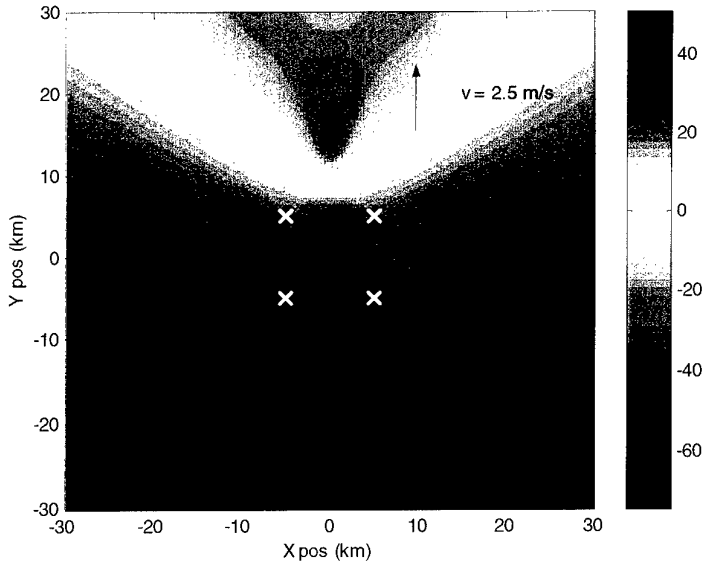

Figure 5 *Error function, in dB re 1Hz, as a function of target position.*

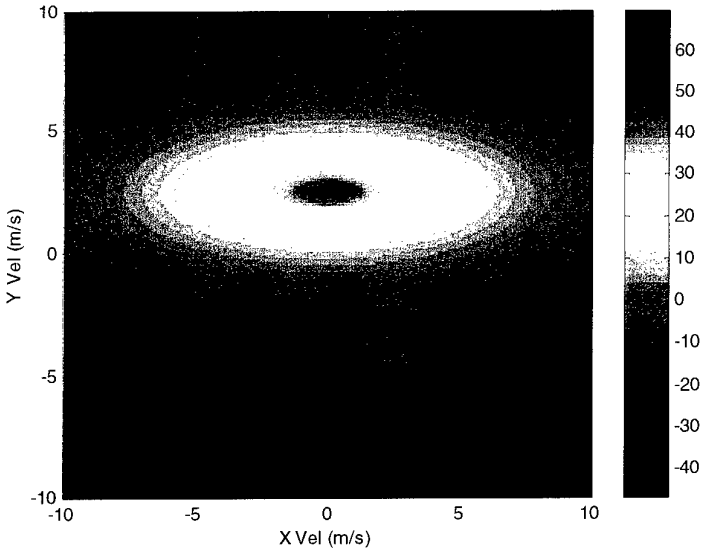

Figure 6 *Error function, in dB re 1Hz, as a function of target velocity.*

Numerical issues

The state vector of the target is determined by minimizing the error function.

The *fmins* function used is part of the MATLAB toolbox. It performs unconstrained minimization of a scalar function of many variables, using the Nelder-Mead simplex method [12]. This method creates a simplex, an N+1-point geometrical figure and its interconnecting segments, where N is the dimensionality of the space. Then, through a set of reflections and contractions it converges on the minimum.

Initially, the following state vector format was used:

$$state = [x, y, speed, bearing]. \tag{9}$$

This was selected because speed-bearing information is more concrete to a system operator than x-y velocity. However, this creates a mathematical problem in the sense that the 4-D space becomes periodic along the bearing axis and symmetric by reflection. Negative speed is positive speed with a bearing offset of 180°. The routine is rendered useless. Hence, the state vector was modified to be truly Cartesian, in order to eliminate this ambiguity:

$$state = [x, y, v_x, v_y]. \tag{10}$$

Also, the *fmins* routine requires an initial, or estimate, vector. A carefully selected estimate must be provided if the routine is to work correctly. The search must not begin at the origin of the plane, for the initial simplex will not be large enough, probably excluding the actual minimum. The estimate vector should be non-zero and of the scale of the problem – distances of the order of a kilometre and speeds of m/s scale.

3
Number of sensors

The number of sensors to be used is an important parameter to be determined. The problem is, in theory, determined by four equations. This means using a minimum of four sensors. Using the minimization routine, grid searches were run for many different numbers of sensors, from three to ten. The underdetermined three-sensor case was run to see if a minimization solution could be found regardless of the lack of information.

3.1 Description of the numerical experiment

Grid searches were simulated within an area of 60 × 60 km, with 1 km resolution. The selected target velocity was 2.5 m/s, a typical value for submarines and surface ships, around 5 kn. The velocity direction was 38° from north, y-axis, a randomly selected value that does not create ambiguities in the error function. Sound speed was set at the accepted average of 1490 m/s and assumed constant. The central frequency was 1 kHz, a typical frequency for active systems.

The search code scanned the grid and performed a minimization at each point. Statistics were computed for accuracy on position, speed and velocity bearing. Accuracy of position is an absolute measure of the distance separating the target found and the true target. Accuracy of speed is the difference between true and found speed. Directional accuracy on the target velocity is the absolute difference between bearing found and true bearing.

For the number-of-sensors study, searches were performed for $N = 3$ to 10. Sensors were placed on a circle of 15 km radius.

3.2 Results

The over-all mean accuracy on position is higher than acceptable, due to the fact that the minimization routine cannot perform the localization in certain blind areas, in this case outside the area delimited by the sensors. Thus the simulation supplies a falsely large value. However, localization accuracy to within 10 m (on a 15 km scale) is readily observed within the area delimited by the sensor layout. The same observations are true for accuracy of speed and velocity bearing. Mean accuracy is therefore computed solely inside the grid confined by the sensor layout.

The error of position, speed and velocity bearing is much higher for the three-sensor configuration than for all other values of N, as was expected because of the underdetermined problem. The triangle configuration never finds the target state vector with precision, i.e., the minimum error is never null. Consequently, localization cannot be performed using only 3 sensors.

For other values of N, the results are consistent. The mean position accuracy is somewhat high, but this is caused by the fact that there are erroneous values in the vicinity of the sensors.

Figure 7 shows the area within which each configuration can perform localization. The area of accuracy is defined as the total area in which the localization is performed to a certain tolerance. In this case it is plotted against the number of sensors. Tolerance in all cases is 100 m on target position, 0.1 m/s on target speed and 5° on velocity bearing. In the circular configuration considered, little is gained by adding more sensors.

Figure 8 shows how the target position error, in kilometres, varies as the number of sensors is increased. Figure 9 illustrates the target speed error, in m/s and Fig. 10 plots velocity bearing error. Sample error plots for $N = 6$ are included, in which the error is plotted in colour with the appropriate scale. The white crosses indicate the platforms.

Note that the suggestions here are based on ideal, perfectly known, sensor locations.

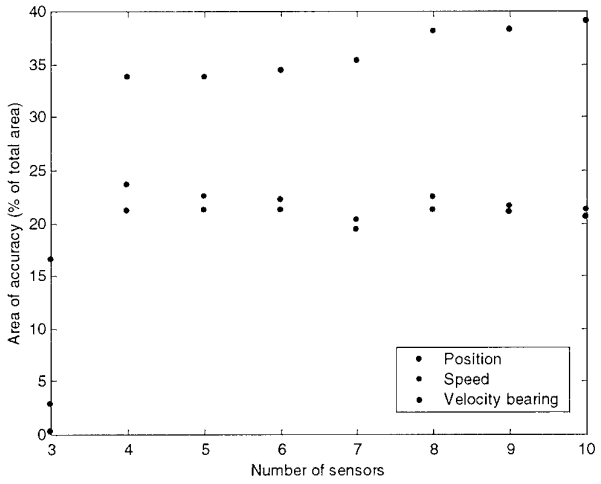

Figure 7 *Area of acceptable accuracy as a function of the number of sensors.*

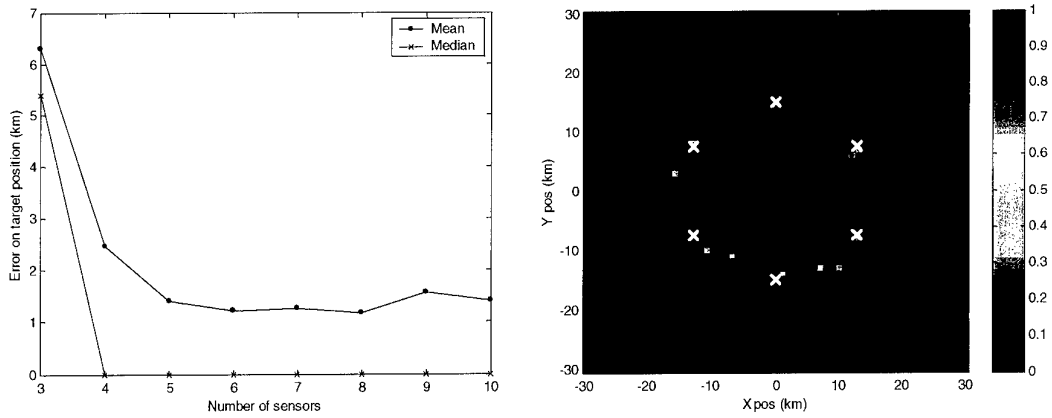

Figure 8 *a) Mean error on position for a target within the sensor grid, as a function of the number of sensors. b) Sample error plot for N=6, colour scale in km.*

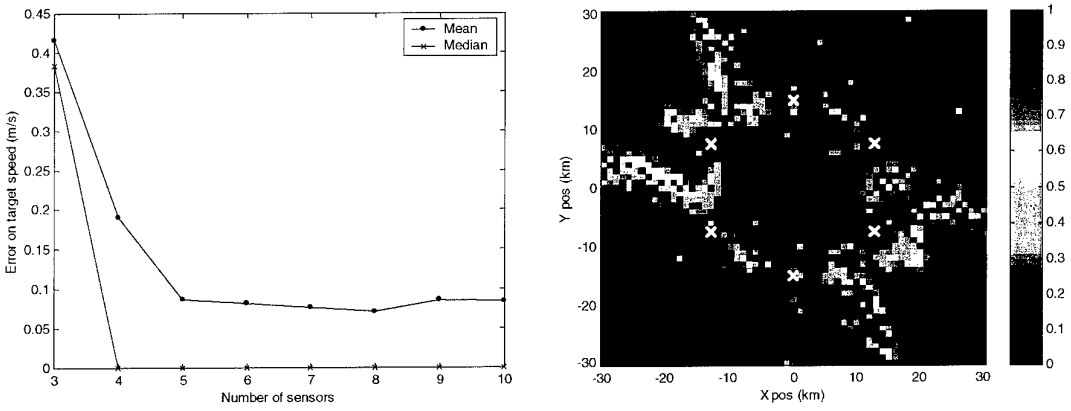

Figure 9 *a) Mean error on speed for a target within the sensor grid, as a function of the number of sensors. b) Sample error plot for N=6, colour scale in m/s.*

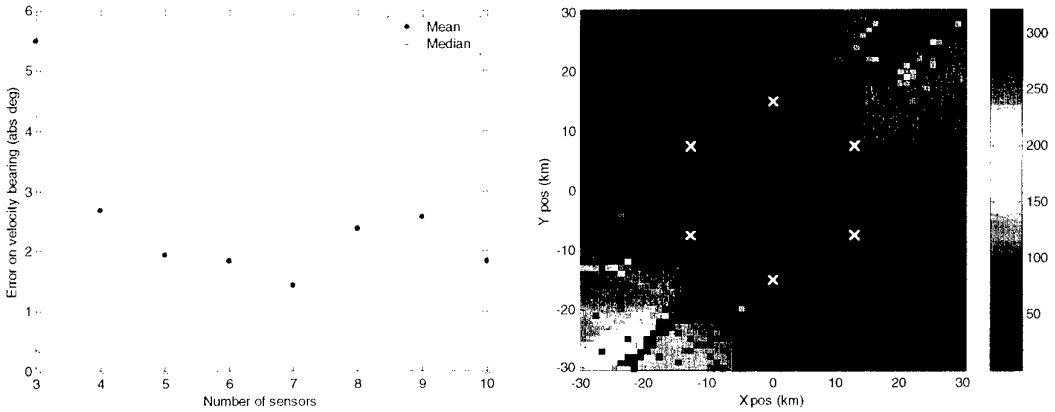

Figure 10 *a) Mean absolute error on velocity bearing for a target within the sensor grid, as a function of the number of sensors. b) Sample error plot for N=6, colour scale in degrees.*

4
Geometry

As it had been determined that configurations of 4 and 6 sensors offered the best performance-to-number-of-sensors ratio, numerical experiments were performed using different sensor configurations. Using four platforms, square, line, L-shape (line with one sensor offset creating a right angle) and uniform random distribution were evaluated. Using six-sensor configurations rectangle, regular hexagon, line, L-shape (with two offset sensors) and uniform random distribution were evaluated.

4.1 Description of the numerical experiment

The numerical experiments consisted of the same simulated grid search as the study on the number of sensors, presented in 3.1. The parameters used were the same: sound speed, 1490 m/s, initial frequency, 1 kHz. The search algorithm was made to search for a target of given position with the same specific velocity, 2.5 m/s at 38° from north.

4.2 Results

Directional dependence

In comparing different configurations, a strong directional dependence has been observed in the square layout. The accuracy of the search depends on target movement direction (target velocity bearing), when the sensors are laid out in a square. In both cases, target velocity is 2.5 m/s at 38° from north. For the first configuration, (Fig. 11a), the area of accuracy for position is 786 km^2, while in Figure 11b the value is 878 km^2. Note the difference in the shape and distribution of the area where the precision is acceptable.

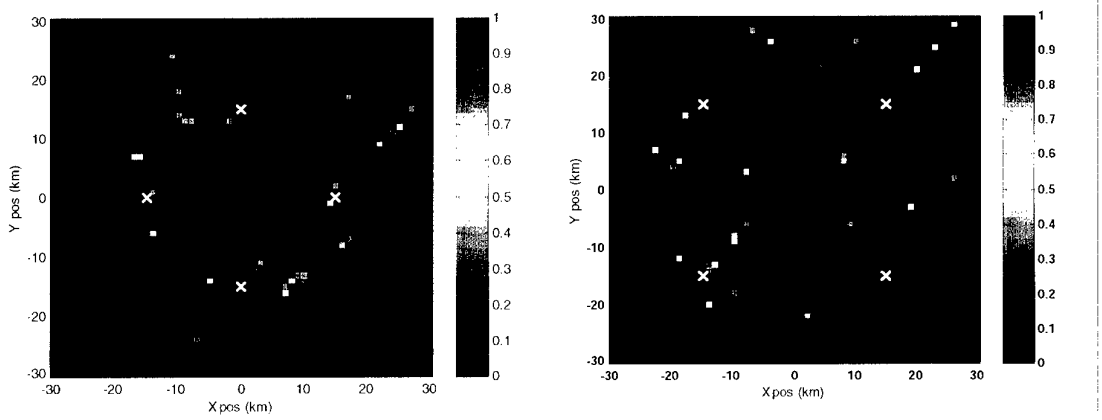

Figure 11. *a) & b) Sample error plots showing the directional dependence of localization.*

Results for different layouts

Table 1 *Area of accuracy for different platform layout configurations.*

Configuration	*Area of accuracy (% of total area)*		
	Position	*Speed*	*Velocity bearing*
4-point			
Square	23.6	26.5	34.5
Line	28.7	44.3	46.1
L-shape	29.8	31.3	39.5
Random distribution	29.1	30.6	42.8
6-point			
Hexagonal	20.6	21.5	34.1
Square	33.2	33.9	43.5
Line	52.4	53.4	55.2
L-shape	41.9	42.5	50.9
Random distribution	35.0	35.3	40.8

Tolerances: position = 100 m, speed = 0.1 m/s, velocity bearing = 5°.

The following pages show plots of localization error on target position and velocity bearing as a function of position. The white crosses indicate the sensors. Colour scale is in kilometres for position error and in degrees for directional error.

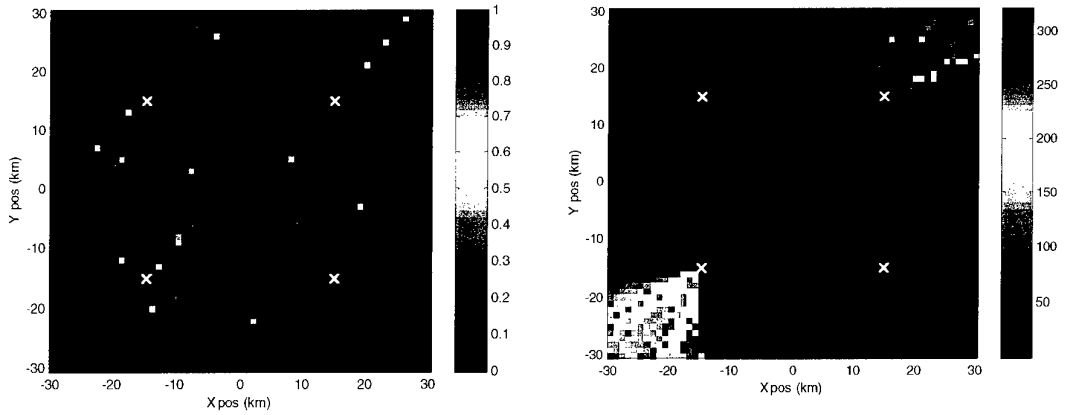

Figure 12 *Error on target position and velocity bearing for the 4-point square configuration. Colour scales are in kilometres and degrees respectively.*

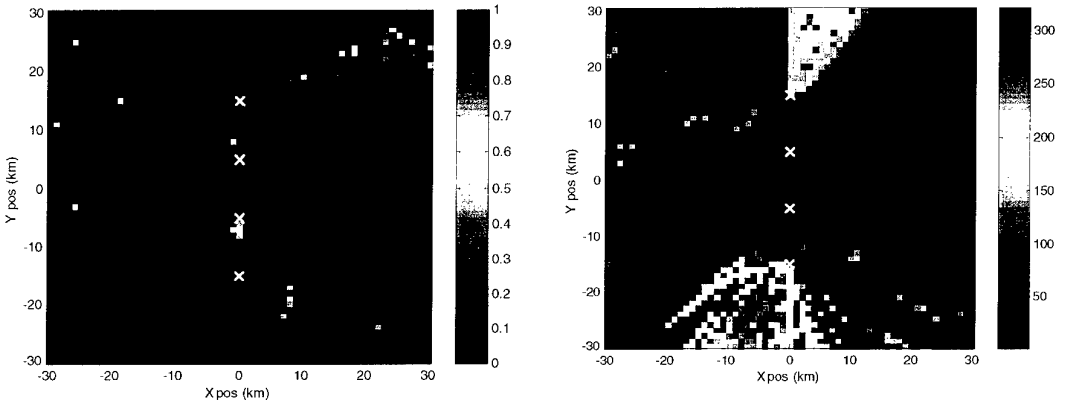

Figure 13 *Error on target position and velocity bearing for the 4-point line configuration.*

The square configuration (Fig. 12) demonstrates poor results on position and velocity bearing localization. The linear configuration (Fig. 13) yields better results, but this is a test performed with one velocity vector. A strong directional dependence is expected with this type of configuration. However, in a barrier/net operation this configuration would be

good for detecting approaching targets with restrained movement capability (by a land mass for example).

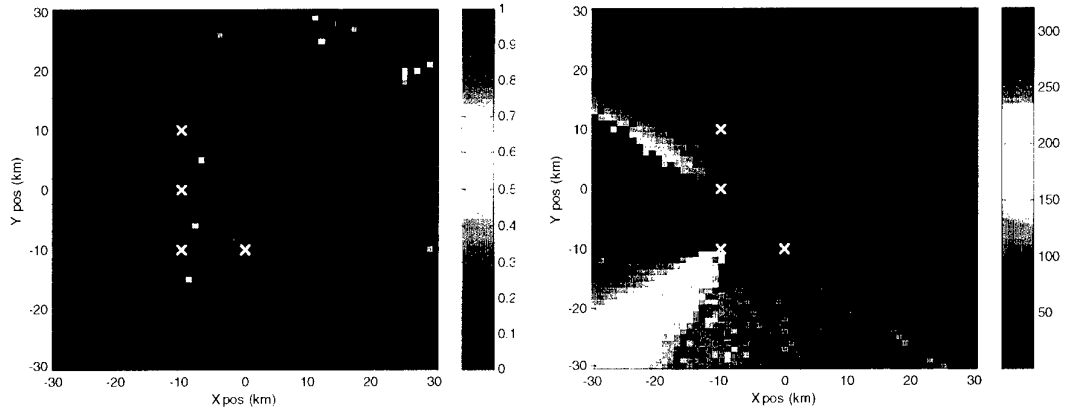

Figure 14 *Error on target position and velocity bearing for the 4-point l-shape configuration.*

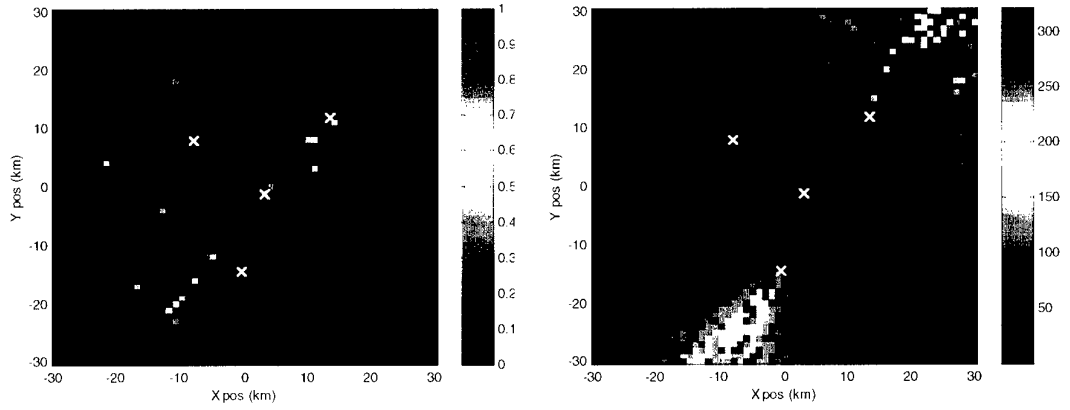

Figure 15 *Error on target position and velocity bearing for a 4-point random distribution of sensors.*

The L-shape configuration (Fig. 14) demonstrates worse results than the linear configuration with regards to area of accuracy. However, the blind area is more easily

defined in the case of the L-shape (Fig. 14). The random distribution of sensors, shown in Fig. 15, is the worst of all cases. Fully randomized distribution should be avoided.

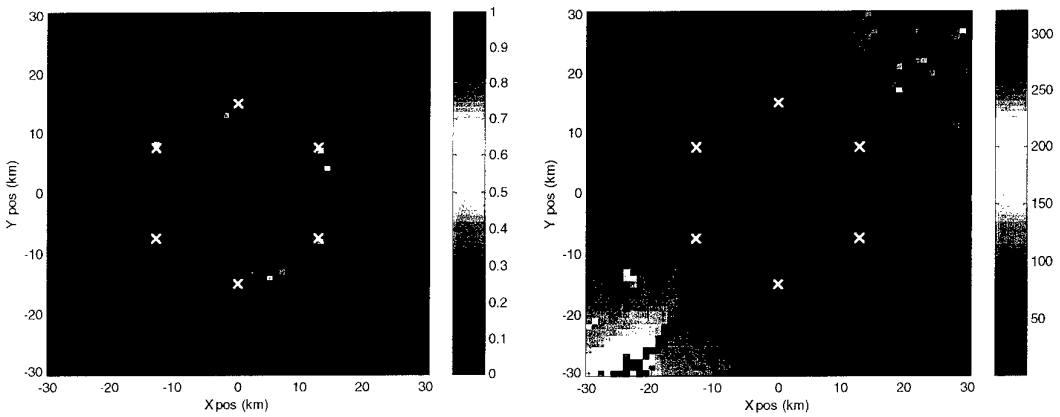

Figure 16 *Error on target position and velocity bearing for the 6-point hexagonal configuration. Colour scales are in kilometres and degrees respectively.*

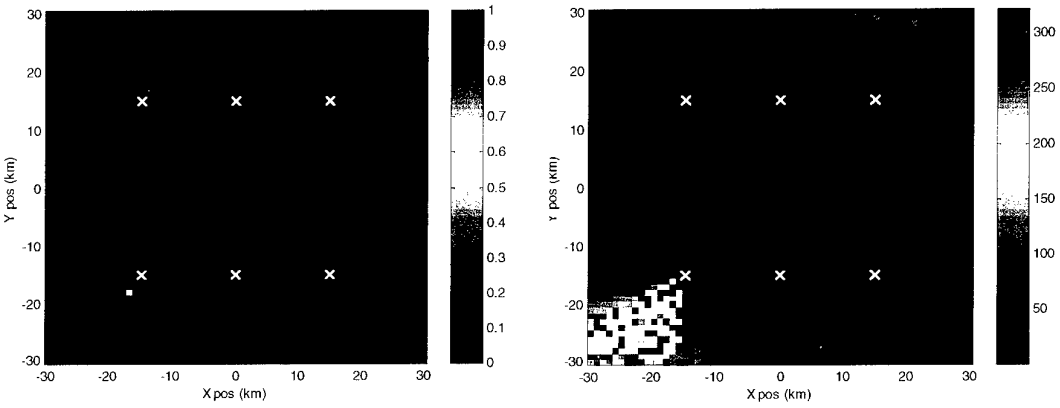

Figure 17 *Error on target position and velocity bearing for the 6-point square configuration.*

The results for the hexagonal configuration are exact inside the polygon, but the localization fails outside (Fig. 16). Extending the diameter of the layout may increase the area covered by the system. The square configuration shows strong directional

dependence: the two extra sensors help to extend the area of accuracy at the centre of the system.

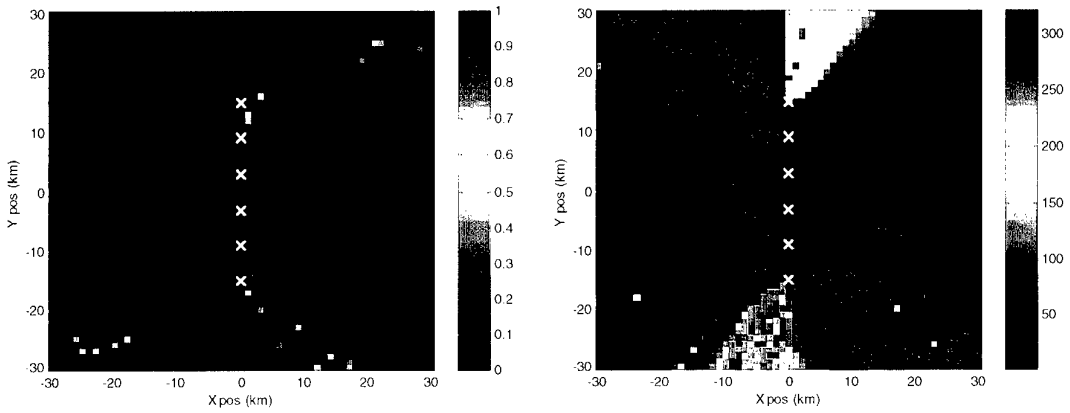

Figure 18 *Error on target position and velocity bearing for the 6-point line configuration.*

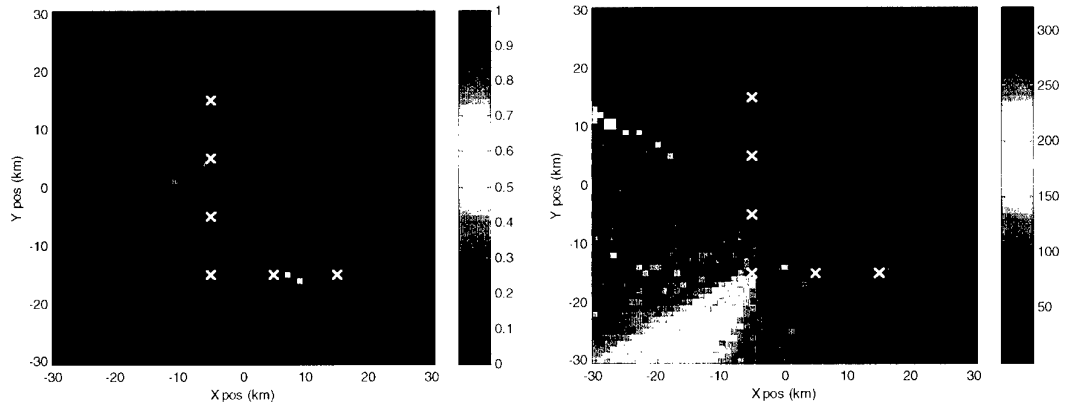

Figure 19 *Error on target position and velocity bearing for the 6-point l-shape configuration.*

The results for the linear configuration do not significantly increase with the addition of 2 sensors and the area of accuracy maintains its shape, (Fig.18). The L-shape configuration does gain from the addition of two sensors. The blind area in the upper-right is eliminated, making this addition viable.

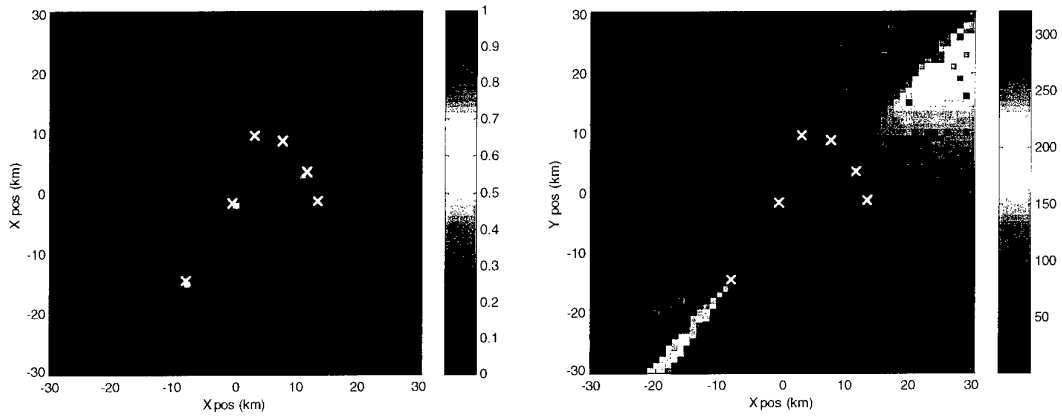

Figure 20 *Error on target position and velocity bearing for a 6-point random distribution.*

Again, the random distribution performs poorly. This was to be expected, as the addition of 2 randomly placed sensors will not logically improve the situation.

The most interesting results were obtained using the L-shape with 6 sensors. A predictable blind area, located behind and near to the sensors, high accuracy and area of accuracy on all variables makes this layout a potential candidate for further study. Strong results were also obtained from the hexagonal layout, although the area of accuracy was small, it must be considered that the blind area is predictable, located outside the sensor layout.

Further tests should be conducted to determine the directional dependence of each of these configurations.

5
Positioning accuracy

In this section, the focus turns to the influence of the position accuracy of the sensors. Previously, all sensor positions were known exactly. At this point, the positions are perturbed in order to simulate a more realistic situation, by introducing normally distributed random perturbation to the sensor positions.

5.1 Description of the numerical experiments

The 4- and 6-point circular layouts were selected for this study. Parameters for the grid searches were maintained from the previous sections. Target velocity was 2.5 m/s at 38° from north. Perturbations were introduced randomly with a normal distribution, equally on all sensors. Values used for variance were 1, 10 and 100 m. The same grid searches were performed 20 times, each with a different perturbation and the results were averaged. For unequal perturbation, the 4-point configuration was selected. One sensor was perturbed with variances of 1, 10 and 100 m, while the others were perturbed with 1 m variance.

5.2 Random perturbation – all sensors equal

Error! Reference source not found. presents the results of the grid search simulations for different values of sensor perturbation. A large decrease in area of accuracy is observed in ***Table*** and in Fig. 21. It illustrates position error for the 6-point configuration, with variance of 0, 1, 10 and 100 m.

Perturbations in sensor position accuracy introduce large errors in target position and speed. 1 m and 10 m perturbations do not significantly hinder the average position and speed results, but they do diminish the area within which accuracy is high. However, when a 100 m perturbation is introduced, the 4-point configuration is unable to perform localization. Target velocity bearing is only slightly affected, with an error of 0.1° being introduced by a 100 m perturbation.

System performance when faced with position uncertainty depends quite strongly on the number of sensors. Where the 4-platform layout fails, the 6-platform system keeps working. Note that in general, in Table 2, the error obtained using 6 sensors is half of that obtained using 4 sensors. However, the area of accuracy is fairly equal, thus much less dependent on N (Table 3).

Table 2 *Average target localization error within the sensor grid, according to variance of sensor perturbation.*

Configuration	Perturbation variance (m)	Average error		
		Position (km)	Speed (m/s)	Velocity bearing (deg)
4-point	0	2.46	0.19	2.68
	1	2.52	0.20	2.57
	10	2.44	0.19	2.61
	100	N/A	N/A	N/A
6-point	0	1.20	0.08	1.83
	1	1.28	0.09	1.96
	10	1.32	0.09	2.01
	100	1.38	0.09	2.08

* N/A indicates inability to perform localization. Tolerances: position = 100 m, speed = 0.1 m/s, velocity bearing = 5°.

Table 3 *Area of accuracy on localization according to variance of sensor perturbation.*

Configuration	Perturbation variance (m)	Area of accuracy (% of total area)		
		Position	*Speed*	*Velocity bearing*
4-point	0	21.1	23.6	33.8
	1	18.9	22.6	33.8
	10	14.5	20.0	32.0
	100	N/A	N/A	N/A
6-point	0	21.3	22.1	34.3
	1	18.9	20.3	33.2
	10	14.9	17.8	31.3
	100	8.2	14.0	26.0

* N/A indicates inability to perform localization. Tolerances: position = 100 m, speed = 0.1 m/s, velocity bearing = 5°.

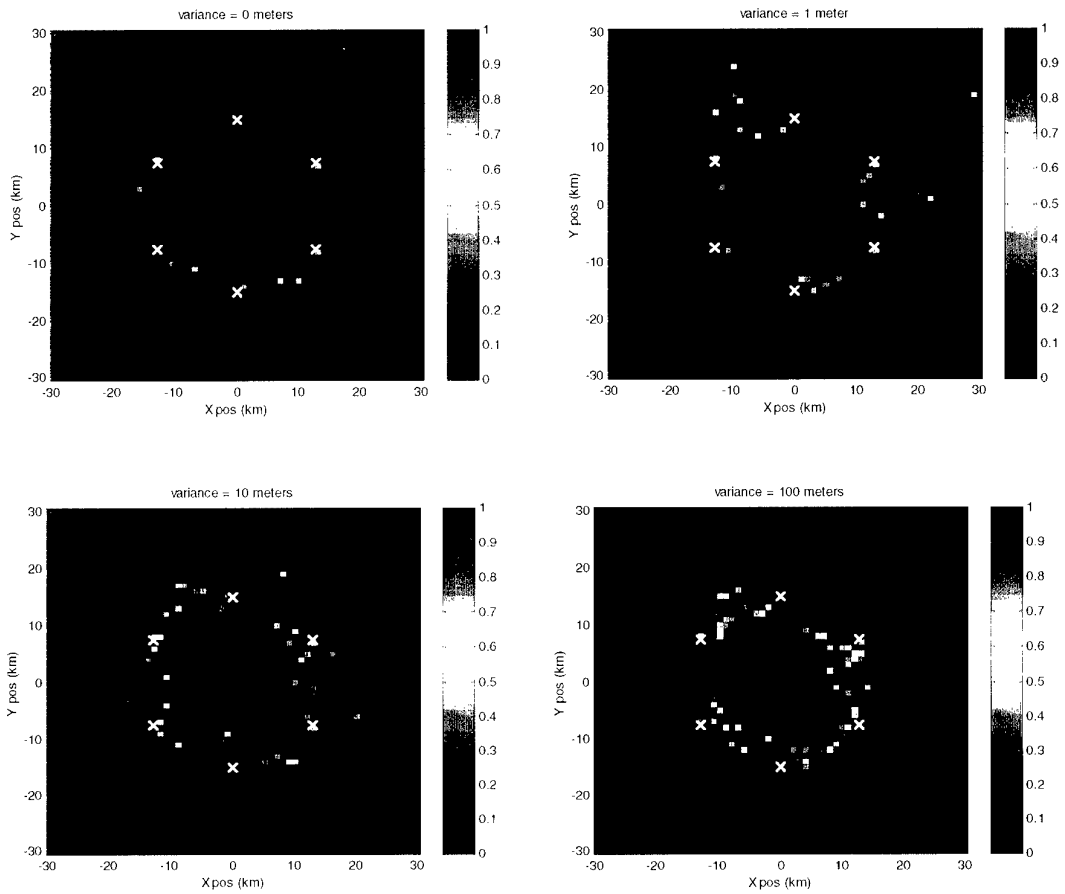

Figure 21 *Target position localization error, for sensor perturbation variances of 0, 1, 10 and 100 m. Colour scale in kilometres.*

5.3 Random perturbation – one sensor different

For the unequal sensor perturbation study, the 4-sensor platform was used.

Table 4 *Average target localization error within the sensor grid, with sensors perturbed unequally.*

Single sensor perturbation variance (m)	Average error		
	Position (km)	Speed (m/s)	Velocity bearing (deg)
1	2.52	0.20	2.56
10	2.5311	0.2019	3.6673
100	N/A	N/A	N/A

* All other sensors perturbed by 1 m. N/A indicates inability to perform localization. Tolerances: position = 100 m, speed = 0.1 m/s, velocity bearing = 5°.

Table 5 *Area of localization accuracy according to variance of single sensor perturbation.*

Single sensor perturbation variance (m)	Area of accuracy (% of total area)		
	Position	*Speed*	*Velocity bearing*
1	18.9	22.6	33.8
10	16.9	21.6	33.3
100	N/A	N/A	N/A

* All other sensors perturbed by 1 m. N/A indicates inability to perform localization. Tolerances: position = 100 m, speed = 0.1 m/s, velocity bearing = 5°.

The perturbation of one sensor influences the results quite strongly (Table 4 and Table 5). Figure 22 illustrates the target position error. The sensors indicated by the white crosses are perturbed by 1 metre and the single sensor (represented by a circle) is perturbed with variances of 1, 10 and 100 m. Some skewing of the results is observed, but it is unclear if this is due strictly to the unequal perturbation or to directional dependence.

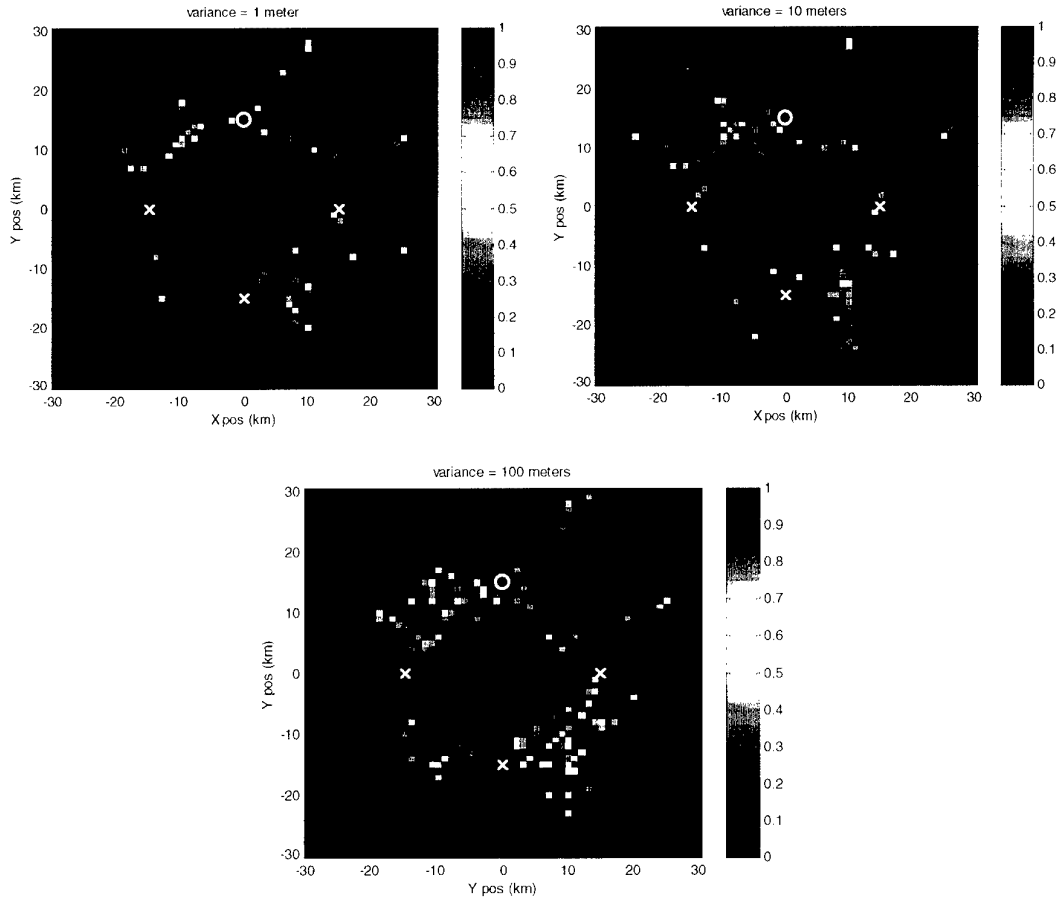

Figure 22 *Error plots on target position localization, with unequal sensor perturbation. Colour scale in kilometres.*

Further investigations should concentrate on improving understanding of the influence of the number of sensors used, on localization. Tests could be conducted on the case where a bias exists in platform position, such as all platforms drifting uniformly.

6
Doppler information accuracy

The influence of perturbations in the data collected by the system is considered. Noise is added to the numerically simulated Doppler information and its effect on localization is studied. The noise is simulated by normally distributed random perturbations.

6.1 Description of the numerical experiment

The simulations were run as in the sensor position accuracy study. In this case, random perturbations were introduced into the Doppler information to simulate a more realistic situation, where noise is present in the collected data. The perturbations were introduced as a percentage of the Doppler information, with variances of 5% and 10%. Multiple grid searches were performed on a target with velocity of 2.5 m/s at a 38° angle to north. Other parameters (sound speed, resolution and output frequency) were unchanged.

6.2 Results

The addition of noise to the Doppler information was found to have the most influence on the results for target speed. Increased errors were also observed for target position and velocity bearing. However, the influence on position and velocity bearing error is negligible in comparison to the error increase in target speed determination. As seen in Table 6, position error fluctuates within 50 m with 5% and 10% noise perturbation; velocity bearing error varies by 0.1°; and the error in determining target speed triples with 10% noise. Table 7 presents the results on area of accuracy achieved. The area of accuracy for position drops by 50% with the addition of noise, but stabilizes as the noise increases. Velocity bearing shows the same decrease followed by stabilization. More interesting is the reduced area of accuracy on target speed. With 10% noise, the search code is unable to achieve the desired tolerance of 0.1 m/s.

Table 6 *Average target localization error within the sensor grid, as a function of Doppler information perturbation.*

Doppler information perturbation (% of true shift)	Average error		
	Position (km)	Speed (m/s)	Velocity bearing (deg)
0	1.26	0.08	1.92
5	1.22	0.17	1.85
10	1.24	0.26	1.85

Table 7 *Area of localization accuracy according to variance of Doppler information perturbation.*

Doppler information perturbation (% of true shift)	Area of accuracy (% of total area)		
	Position	*Speed*	*Velocity bearing*
0	20.6	21.4	34.0
5	9.5	4.8	24.2
10	9.2	0	23.7

Tolerances: position = 100 m, speed = 0.1 m/s, velocity bearing = 5°.

Figure 23 plots the error on target speed, illustrating the change in accuracy with the addition of noise. White crosses indicate sensors and colour scale is in metres per second.

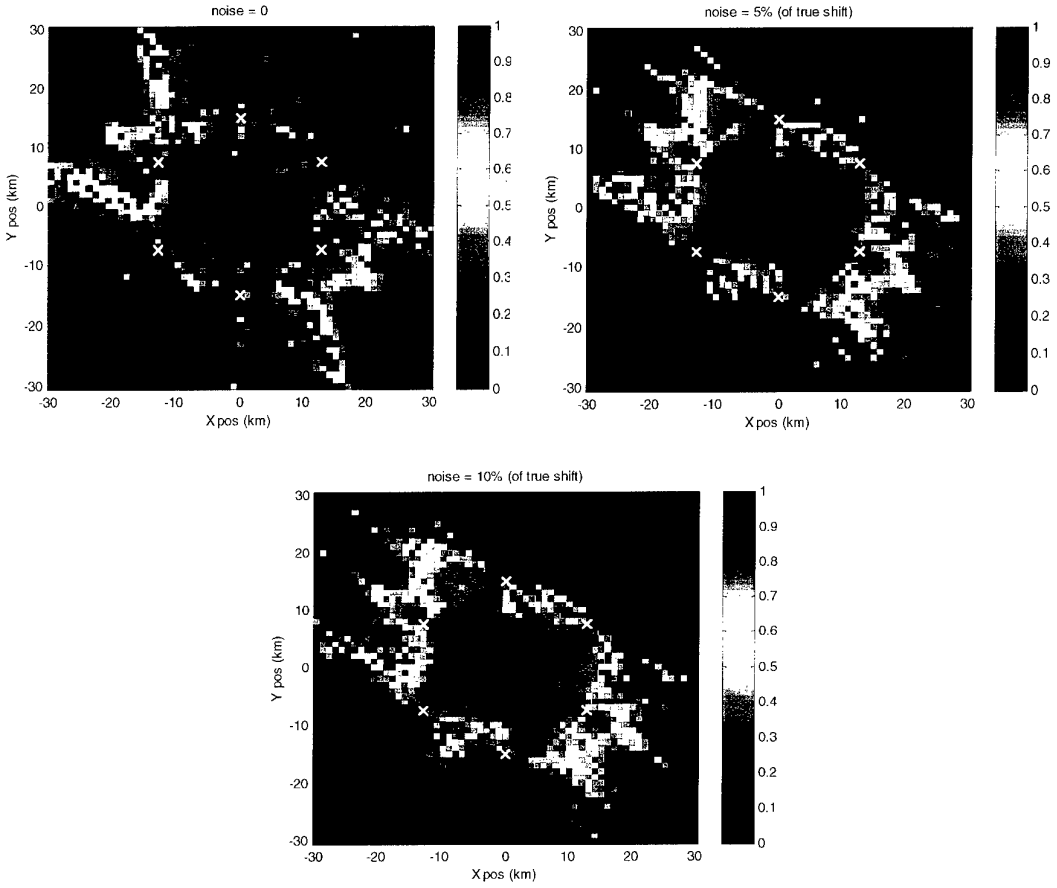

Figure 23 *Error plots on target speed, with different Doppler shift noise values. Colour scale in metres per second.*

The results are gradually degraded by perturbations in the Doppler information, rather than decreasing the area of accuracy as in the sensor position uncertainty study of Section 5. This is illustrated in Fig. 23, where the area within the sensors becomes gradually lighter, indicating greater error.

An interesting case for further study would be to evaluate the influence of quantization of the Doppler information in order to simulate a realistic sampling situation.

7

Single-source configuration

In the passive sonar situation, the initial frequency becomes a variable, bringing the total to five. The analytic solution then requires, in theory, five equations. Therefore, the number of sensors must also be augmented to a minimum of five in order to supply sufficient information to completely determine the problem. This drawback is compensated for by the fact that an active source is not needed.

The active sonar situation requires that the initial frequency is known. This simplifies the problem. Two different systems can be proposed for the active case: multiple source-sensor platforms and multiple sensor-only platforms coupled with a single source.

In the multi-source case, the frequency information received by each sensor is shifted by twice the single-propagation Doppler described in Eq. (5), provided the target and sensor velocities are small compared to c, (Sections 3-6).

In the single source case (Fig. 24) the Doppler shift affecting the signal is in two parts. As the impulse travels from the source to the target, it is affected by a shift proportional to the source-target range variation rate. After reflection, the impulse is affected by a frequency shift proportional to the target-sensor range variation rate. The system consists of a single source (which can also be a receiver) and N sensors.

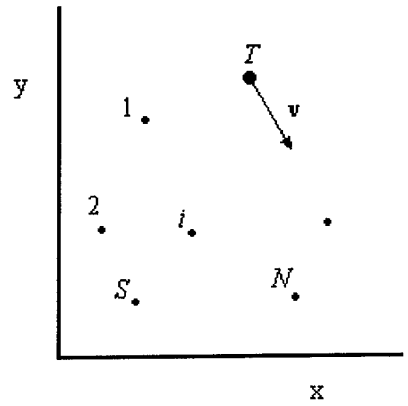

Figure 24 *Single-source problem.*

The total shift is the sum of two equations of type (5):

$$\Delta f_{Doppler} = -\frac{f_{source}}{c}\left[(\vec{v}_T - \vec{v}_S)\cdot \hat{u}_{ST} + (\vec{v}_T - \vec{v}_R)\cdot \hat{u}_{RT}\right] \quad (11)$$

The vector system used in Eq. (11) is presented in Fig. 25, [13].

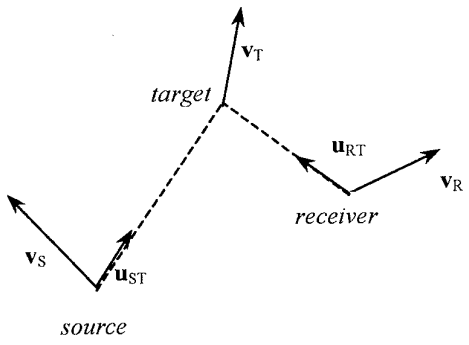

Figure 25 *Bi-static Doppler shift situation: source, target and receiver.*

7.1 Description of the numerical experiment

In order to investigate the performance of the single-source configuration, single grid searches were run for different configurations of 4 and 6 sensors. In both cases, tests were performed with the source combined with one of the sensors and with the source independent from the sensors. Thus, 4 different combinations were evaluated. The platform positions and Doppler information were left unperturbed. In the separate source case, the source position was selected randomly within the receiver grid. Other parameters were the same as in previous sections.

7.2 Results

Table 8 shows the results obtained from each configuration. The best results were obtained using a 6-point receiver layout, with a source positioned independently. Better results were obtained using a separate source rather than one combined with a sensor. In comparison with the multiple sensor system, the area of accuracy is smaller when using a single source. However, little decrease in performance is observed when selecting a single-source system. The decrease in cost of the system justifies the slight sacrifice in performance.

Table 8 *Area of accuracy obtained from different single-source configurations.*

Configuration	Area of accuracy (% of total area)		
	Position	*Speed*	*Velocity bearing*
4-point, multiple source	21.1	23.6	33.8
4-point, combined source	17.7	19.3	33.7
4-point, separate source	19.1	20.6	33.1
6-point, multiple source	21.3	22.1	34.3
6-point, combined source	16.5	17.3	30.6
6-point, separate source	20.3	21.0	37.1

Tolerances: position = 100 m, speed = 0.1 m/s, velocity bearing = 5°.

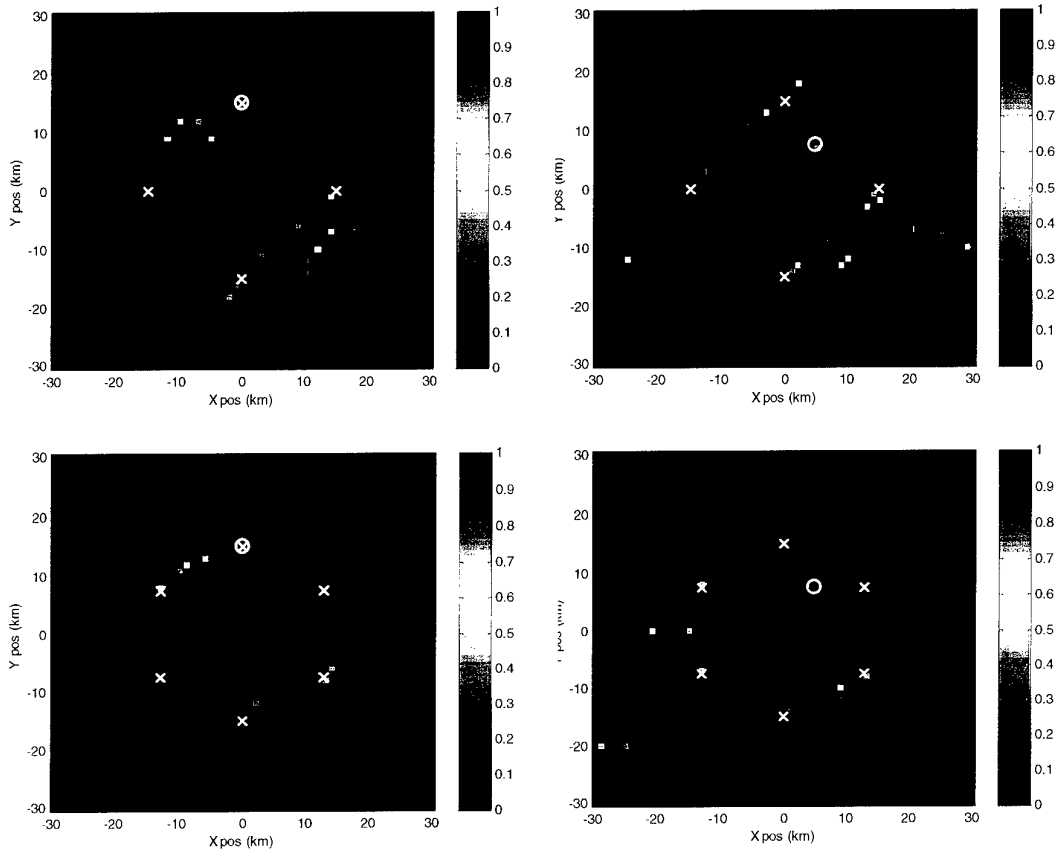

Figure 26 *Target position localization error, for each single source configuration considered. Colour scale in kilometres.*

This preliminary study of single-source systems opens the door to many possibilities worth investigating. Primarily, this type of system is of interest as it requires only one source. Results show that using a source independent from the sensors improves the results, thus creating the possibility of using less-expensive stand-alone sources and receivers rather than more complicated combined platforms. Furthermore, in a realistic situation the bistatic characteristic of such a system eliminates the capability of a submarine to minimize its target strength by *turning its tail* to the source.

Further studies could combine single-source configurations with different configurations (such as in Section 4) and also the use of separate sources. The influence of sensor position uncertainty and noise in Doppler information should also be evaluated (Sections 5 and 6). The passive case is also worth investigating, as it incorporates the concomitant advantages of a quiet system.

8
Conclusions

8.1 Discussion and summary

This time-limited feasibility study was meant to shed light upon the issues concerning Doppler-only localization. This problem is important in resolving target position and velocities using CW or narrow-band multiple platform systems.

The problem was formulated analytically and the numerical method used to solve it was presented. An analytical solution being too complicated, numerical methods were used, although a semi-analytical solution was developed (Annex A). The method used minimizes an error function of the Doppler shift. Through an unconstrained Nelder-Mead simplex minimization routine, the search code attempts to locate the target and determine its velocity. Comments on state-vector definitions and estimate vector selection are included.

The work focused on the number of sensors to be included. The average error and area of accuracy were evaluated for values of N from 3 to 10. The underdetermined 3-point search failed, as was expected. The area over which localization can be performed is usually clearly defined, with the drop being roughly step-like. The addition of sensors does not increase this area of accuracy with the particular circular geometry considered. Nonetheless, the average error within the sensor grid improves by 50 % when going from $N = 4$ to $N = 6$.

Different configurations were investigated. The best results were obtained using lines and L-shapes, keeping in mind that great directional dependence was observed. In the case of the L-shape, increasing the number of sensors from 4 to 6 improved the results by 10 percentage points, while eliminating a large blind area (compare Fig. 14 and Fig. 19). Fully randomized distribution and "perfect" symmetry were avoided. Certain configurations produce a predictable blind area.

The influence of sensor position uncertainty on the results of the localization was evaluated. The 4-point configuration was greatly affected by uncertainty and was unable to perform localization with an uncertainty of 100 m. When using 6 sensors, localization was still possible, but with a 25 to 50% decrease in area of accuracy for a 100 m uncertainty, depending on the target state variable considered. Furthermore, the mean error on position obtained with the 6-point layout is roughly half of that obtained with 4 sensors. The 6-point configuration was found to stand up better to sensor position uncertainty. Unequal perturbations were also investigated, with the 6-point yielding better results yet again.

The presence of noise in the Doppler information was also studied. It was found to have slight influence on position error and velocity bearing error, but a greater influence on target speed computation. Noise increases the error gradually over the whole accuracy area, rather than diminishing the area itself.

Finally, a different data collection system was considered. Instead of multiple source-receiver platforms, a single-source system was considered. The error results were found to increase only slightly. The area of accuracy drops by a few percentage points when switching from multiple-source to single-source. The decrease in expense of such a system would compensate for the slight decrease in accuracy.

8.2 Suggestions for future work

This project has created more questions than answers. Follow-up work should treat many different subjects. Ideally, one could seek a closed-form or partially closed-form solution, if not only for a particular case (single-source, specific geometry). Work on the confined target solution in Annex A would also be useful. The single-source active problem in Section 7 has raised interesting questions that should be answered. The passive case should also be considered.

The directional dependence of the different configurations observed in Section 4, should be studied in order to characterize them for specific real-life situations. Knowledge of the effects of Doppler information quantization would also be of use to simulate real systems, as suggested in Section 6. This study has considered the problem at one scale: varying the scale and dimensions of the problem could bring about interesting results.

An improved minimization routine, possibly a constrained minimization could be of some help.

This project was completed using MATLAB for numerical simulations, [14]. Code developed in the course of this project is available from SACLANTCEN.

9 Acknowledgements

I would like to thank Dr. Joseph E. Bondaryk, project supervisor and co-author, for all of his help and advice throughout the course of this study. His guidance made it possible to overcome the problems I encountered.

Sincere regards also to Dr. Jochen Ziegenbein, head of SSD, for supplying the opportunity to work on this project; and finally, to SACLANTCEN for supplying the framework for such a project.

References

[1] Johnson, H.M. Important Issues in Bearings-Only Target Motion Analysis, DSTO-TR-0578. Canberra, Australia, Maritime Operations Division, Aeronautical and Maritime Research Laboratory, Department of Defense, 1987. [AD B 232 127]

[2] Passerieux, J.M. *et al.* Target motion analysis with bearings and frequencies measurements via instrumental variable estimates. *Proceedings of the International Conference on Acoustics Speech and Signal Processing '89*, Glasgow, Scotland, May 1989.

[3] Jauffret, C., Bar-Shalom, Y. Track formation with bearing and frequency measurements in clutter. *IEEE Transactions on Aerospace and Electronic Systems*, **26,** 1990:999-1009.

[4] Chan, Y.T., Rudnicki, S.W. Bearings-only and Doppler bearing tracking using instrumental variables. *IEEE Transactions on Aerospace and Electronic Systems*, **28**, 1992:1076-1082.

[5] Levanon, N. Some results from using Doppler derivatives. *IEEE Transactions on Aerospace and Electronic Systems*, **16,** 1980:727-729.

[6] Webster, R.J. An exact trajectory solution from Doppler shift measurements. *IEEE Transactions on Aerospace and Electronic Systems*, **18**,1982:249-252.

[7] Shensa, M.J. On the uniqueness of Doppler tracking. *Journal of the acoustical Society of America*, **76**, 1981:1062-1064.

[8] Weinstein, E. Optimal source localization and tracking from passive array measurements. *IEEE Transactions on Acoustics, Speech and Signal Processing*, **30**, 1982: 69-76.

[9] Statman, J.K., Rodemich, E.R. Parameter estimation based on Doppler frequency shifts. *IEEE Transactions on Aerospace and Electronic Systems*, **23**, 1987:31-39.

[10] Chan, Y.T., Jardine, F.L. Target localization and tracking from Doppler-shift measurements. *IEEE Journal of Oceanic Engineering*, **15**,1990:251-257.

[11] Johnson, D.H., Dudgeon, D.E. Array Signal Processing, Concepts and Techniques, 1st edition, Englewood Cliffs, NJ, USA, P T R Prentice-Hall, 1993. [ISBN 013-0485-136]

[12] Press, W.H., Teulosky, S.A., Vetterling, W.T., Flannery, B.P. Numerical Recipes in C: The Art of Scientific Computing, 2nd edition, Cambridge, MA, USA, Cambridge University Press, 1992. [ISBN 052-1431-085]

[13] Bradley, M. (1996) Environmental Acoustics Pocket Handbook, 2nd edition, Slidell, LA, USA, Planning Systems Incorporated, 1996.

[14] The MathWorks Inc. MATLAB, The Language of Technical Computing: Using MATLAB, MATLAB user's manual, Natick, MA, USA, 1996.

Annex A

An alternate solution to a particular case: confined target

Consider a target confined to a circular area of radius r. The Doppler frequency shift has a very specific value around the area's border, that can be described by a function $\Delta f_{Doppler}(\theta)$, where θ is the angle to a reference axis, here the x-axis. From this Doppler shift, the rate of variation of the range between the target and the edge of the area can be extracted with Eq. (A.1) for the combined source-sensor problem, or Eq. (A.2) for the single-source, multiple-sensor problem.

$$\Delta f_{Doppler}(\theta) = -\frac{2 f_0}{c} v(\theta) \tag{A.1}$$

$$\Delta f_{Doppler}(\theta) = -\frac{f_0}{c}\left[v_{source \to target} + v(\theta)\right] \tag{A.2}$$

A set of source-sensors is distributed along the circumference of this circle. A sampling v_i of the Doppler shift is obtained. If, by some method of interpolation, the function $v(\theta)$ can be extracted, one can then extract the information when need to perform localization. Thus, the numerical problem is reduced from a four-dimensional minimization to a one-dimensional interpolation of a smooth function. The following shows how the target location and velocity are obtained analytically.

Considering Fig. 27, Eq. (A.3) provides the range rate between the target and any point on the circle (see Eq. (7)):

$$v(\theta) = -\frac{\dot{x}_T (x_T - r\cos\theta) + \dot{y}_T (y_T - r\sin\theta)}{\sqrt{(x_T - r\cos\theta)^2 + (y_T - r\sin\theta)^2}} \tag{A.3}$$

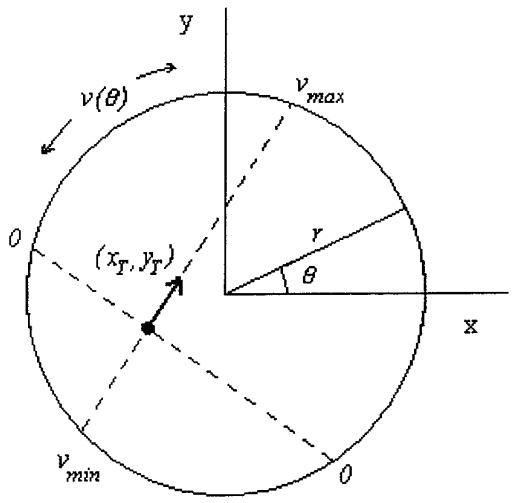

Figure 27 *Confined target problem illustration.*

The sensors are taken to be stationary. An example of Eq. (A.3) is plotted in Fig. 28, with:

$r = 15$, $(x_T, y_T) = (-5, -3)$ and $(\dot{x}_T, \dot{y}_T) = (1, 2)$.

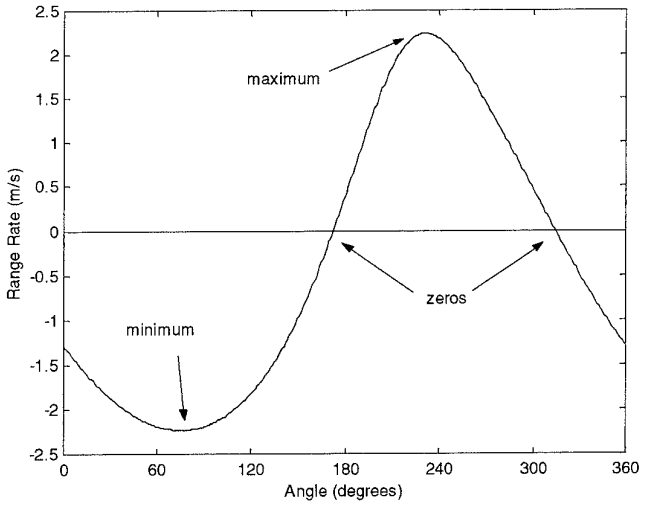

Figure 28 *Range-rate function example, for a given set of parameters.*

From the function presented in Eq. (A.3), one obtains the position of the maximum, the minimum and the zeros, defined below.

$$(x_{\max}, y_{\max}) = (r\cos\theta_{\max}, r\sin\theta_{\max})$$

$$(x_{\min}, y_{\min}) = (r\cos\theta_{\min}, r\sin\theta_{\min}) \tag{A.4}$$

$$(x_1, y_1) = (r\cos\theta_1, r\sin\theta_1)$$

$$(x_2, y_2) = (r\cos\theta_2, r\sin\theta_2)$$

The position of the target is obtained from the intersection of the following linear functions:

$$y - y_{\max} = \left(\frac{y_{\max} - y_{\min}}{x_{\max} - x_{\min}}\right)(x - x_{\max}) \tag{A.5}$$

and,

$$y - y_2 = \left(\frac{y_2 - y_1}{x_2 - x_2}\right)(x - x_2). \tag{A.6}$$

From Eq. (A.5) and Eq. (A.6), one obtains:

$$x_T = \frac{\Delta_m x_m - \Delta_0 x_0 + y_0 - y_{\min}}{\Delta_m - \Delta_0} \tag{A.7}$$

$$y_T = \frac{\Delta_m y_0 - \Delta_0 y_m + \Delta_m \Delta_0 (x_m - x_0)}{\Delta_m - \Delta_0} \tag{A.8}$$

where,

$$\Delta_m \equiv \frac{y_{\max} - y_{\min}}{x_{\max} - x_{\min}}, \qquad \Delta_0 \equiv \frac{y_2 - y_1}{x_2 - x_1} \tag{A.9}$$

and,

$x_m = x_{max}$ or x_{min}, $\qquad y_m = y_{max}$ or y_{min}

$x^0 = x_1$ or x_2, $\qquad y_0 = y_1$ or y_2.

If matrix notation is used, one obtains:

$$\tilde{\Delta} X_T = X_0 \tag{A.10}$$

where,

$$\tilde{\Delta} \equiv \begin{bmatrix} 1 & -\Delta_1 \\ 1 & -\Delta_2 \end{bmatrix}, \qquad X_0 = \begin{bmatrix} y_m - \Delta_m x_m \\ y_0 - \Delta_0 x_0 \end{bmatrix}, \text{ and } \qquad X_T = \begin{bmatrix} x_T \\ y_T \end{bmatrix} \tag{A.11}$$

Target position is obtained by reversing Eq. (A.10).

Target velocity is easily obtained, by determining speed v and direction ϕ:

$$v = v_{\max}, \text{ and } \tan\phi = \frac{y_{\max} - y_{\min}}{x_{\max} - x_{\min}} \tag{A.12}$$

which yields, in x-y velocity:

$$v_x = v\cos\phi, \text{ and } v_y = v\sin\phi. \tag{A.13}$$

Thus, the problem is transformed from a minimization on four variables to an interpolation on a single variable. A circle is used, but an ellipse can also be used, with some modifications to the mathematics. In this particular problem, localization accuracy depends on the quality of the sampling and of the interpolation.

Document Data Sheet

Security Classification		Project No.
UNCLASSIFIED		04-B
Document Serial No.	**Date of Issue**	**Total Pages**
SR-325	July 2000	46 pp.

Author(s)

Levesque, I., Bondaryk, J.

Title

Performance issues concerning Doppler-only localization of submarine targets

Abstract

Target localization can be achieved using only frequency information obtained from source-receiver platforms. The numerical method proposed achieves machine precision accuracy in computing target position and velocity from multiple simultaneous Doppler-shift measurements. The area over which localization can be performed depends very strongly on the configuration in which the sensors are placed, and the drop-off in performance is step-like. A negligible decrease in performance is encountered when switching from "*N*-source, *N*-sensors" to a "single-source, *N*-sensor" configuration. The number of sensors to be used is an important criterion, and it is found that increasing this beyond 4 is only worthwhile with certain configurations. Uncertainties in the sensor locations decrease the area over which accuracy is acceptable; a 10 m uncertainty translates into a 5% loss in coverage. Noise in the Doppler information decreases accuracy gradually; one should expect an error 3 times greater with the addition of 10% noise.

Keywords

Keywords: Localization, Doppler effect, CW systems, narrow-band systems, Doppler-only localization (DOL)

Issuing Organization

North Atlantic Treaty Organization
SACLANT Undersea Research Centre
Viale San Bartolomeo 400, 19138 La Spezia, Italy

[From N. America: SACLANTCEN (New York) APO AE 09613]

Tel: +39 0187 527 361
Fax:+39 0187 527 700

E-mail: library@saclantc.nato.int

The SACLANT Undersea Research Centre provides the Supreme Allied Commander Atlantic (SACLANT) with scientific and technical assistance under the terms of its NATO charter, which entered into force on 1 February 1963. Without prejudice to this main task - and under the policy direction of SACLANT - the Centre also renders scientific and technical assistance to the individual NATO nations.

This document is approved for public release.
Distribution is unlimited

SACLANT Undersea Research Centre
Viale San Bartolomeo 400
19138 San Bartolomeo (SP), Italy

tel: +39 0187 527 (1) or extension
fax: +39 0187 527 700

e-mail: library@saclantc.nato.int

NORTH ATLANTIC TREATY ORGANIZATION